2D Constellation Distortion for Subduing Equalization Noise in Bandwidth-Limited IMDD Systems

Essam Berikaa, *Graduate Student Member, IEEE*, Md. Samiul Alam, *Graduate Student Member, IEEE*, Maxime Jacques, *Graduate Student Member, IEEE*, Xueyang Li, *Member, IEEE*, Ping-Chiek Koh, and David V. Plant, *Fellow, IEEE*

***Abstract*— Bandwidth-limited IMDD systems suffer from the noise boosted by the strong equalization at the receiver. This letter proposes a multiplication-free approach that reduces the impacts of the equalizer-enhanced colored noise through time-interleaving the received symbols and distorting the two-dimensional (2D) constellation such that the noise correlation is subdued. The 2D distortion map is predefined and retrieved from a look-up table. The proposed 2D constellation distortion is evaluated after the linear feed-forward equalizer and Volterra nonlinear equalizer. Experimental results show a BER reduction of 40% when the 2D constellation distortion is employed after the equalizer for the 135 Gbaud PAM4 and 110 Gbaud PAM6 signals. Owing to the proposed approach, we transmit a net data rate of 250 Gbps/λ PAM4 and PAM6 in the O-band over 2 km of SSMF at a BER of 3.8×10^{-3} below the 6.7% overhead HD-FEC using a 47 GHz SiP modulator, linear equalization, and the proposed 2D distortion.**

***Index Terms*— Colored noise, equalizers, intensity modulation, optical interconnections, silicon photonics.**

I. Introduction

THE explosive growth of bandwidth-hungry applications as 4K/8K video streaming, the 5th generation (5G) wireless communication, and cloud computing causes a rapid increase in datacenter traffic, which emphasizes the need to increase the capacity of short-reach optical links and datacenter interconnects (DCI) [1]. Intensity modulation /direct detection (IMDD) systems are employed in short-reach links because of their cost-effectiveness, simple architecture, and power efficiency. Different modulation formats and orders have been investigated in IMDD systems, out of which PAM4 stands out as the optimum solution considering transceiver complexity and power requirements [2], [3]. Thus, the IEEE 802.3bs standard for 400 GbE adopted PAM4 for various distances up to 10 km [4]. The increase in capacity demand indicates the urgency of increasing the data rate per lane from 100 Gbps/λ to 200 Gbps/λ and beyond for next-generation 800 GbE and 1.6 TbE. We have reported the transmission of net 305 Gbps probabilistically shaped PAM8 over 2 km in the O-band; featuring the highest reported throughput using a SiP modulator in IMDD experiment [5]. Recently, record back-to-back transmission of net 402 Gbps PAM8 has been reported using electro-absorption modulated O-band laser (EML) [6]. However, standardizing PAM8 is not anticipated in the near future due to its higher signal-to-noise ratio (SNR) requirements and soft-decision forward error correction (SD-FEC) decoder complexity.

Moreover, the inferior development of components' bandwidth compared to the capacity demand emphasizes the importance of investigating bandwidth-limited IMDD systems. There exist several demonstrations of 200 Gbps/λ IMDD systems using high bandwidth bulk Lithium niobite ($LiNbO_3$) and indium phosphide (InP) modulators; however, both material systems are incompatible with the complementary metal-oxide-semiconductor (CMOS) process flow [7]. On the other hand, silicon photonics (SiP) modulators offer low-cost and large-scale production along with their compatibility with CMOS, which paves their way towards massive deployment [8]. SiP modulators have limited bandwidth compared to $LiNbO_3$ and InP modulators. Hence, increasing the capacity using SiP-modulators requires challenging their bandwidth, and operating in the bandwidth-limited regime. At high symbol rates, bandwidth-limited IMDD systems suffer from the strong intersymbol interference (ISI) that requires powerful equalization at the receiver [9], [10]. However, the powerful equalization amplifies the high-frequency noise within the signal bandwidth and reduces the SNR, which has been reported by several studies and is referred to as equalizer-enhanced in-band noise [11], [12]. This colored correlated noise is handled by adding a post-filter after the equalizer that whitens the noise spectral density at the expense of increasing the ISI. The added ISI is tackled by the maximum likelihood sequence detection (MLSD) algorithm, which adds considerable complexity to the receiver [12]–[14].

This letter proposes a multiplication-free geometric approach that effectively lessens the impacts of the equalizer-enhanced in-band noise and reduces the bit error ratio (BER). The proposed approach distorts the two-dimensional (2D) constellation created from the received signal using a predefined 2D map retrieved from a look-up table (LUT). The effectiveness of the proposed approach is assessed after equalization based on the linear feed-forward equalizer (FFE) and Volterra 3rd order nonlinear equalizer (VNLE), and is compared to the MLSD algorithm. We evaluated the

Manuscript received November 30, 2021; revised January 23, 2022; accepted February 6, 2022. Date of publication February 8, 2022; date of current version February 18, 2022. *(Corresponding author: Essam Berikaa.)*

Essam Berikaa, Md. Samiul Alam, Maxime Jacques, Xueyang Li, and David V. Plant are with the Photonic Systems Group, Department of Electrical and Computer Engineering, McGill University, Montréal, QC H3A 0E9, Canada (e-mail: essam.berikaa@mail.mcgill.ca; md.samiul.alam@mail.mcgill.ca; maxime.jacques@mail.mcgill.ca; xueyang.li@mail.mcgill.ca; david.plant@mcgill.ca).

Ping-Chiek Koh is with Lumentum Corporation, San Jose, CA 95131 USA (e-mail: ping-chiek.koh@lumentum.com).

Color versions of one or more figures in this letter are available at https://doi.org/10.1109/LPT.2022.3150231.

Digital Object Identifier 10.1109/LPT.2022.3150231

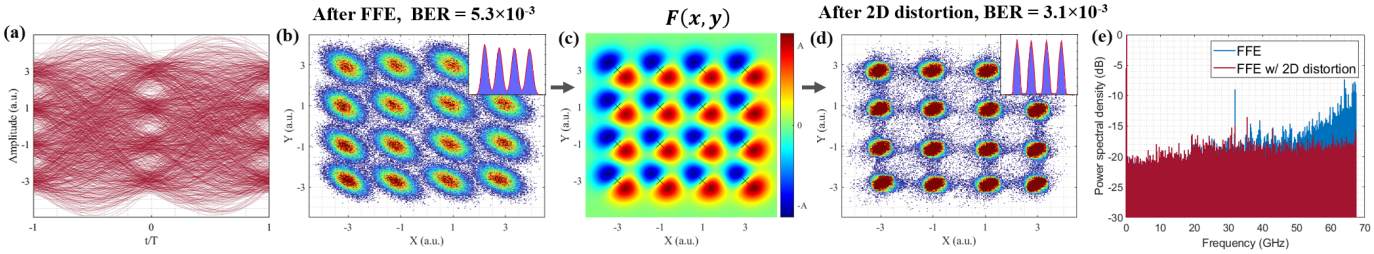

Fig. 1. (a) The received electrical eye diagram after 2 km of 135 Gbaud PAM4 signal, (b) the 2D constellation generated from the same signal after the FFE, (c) the proposed 2D function for constellation distortion, (d) the 2D constellation after distortion, and (e) the noise power spectral density before and after the 2D constellation distortion. The inset histograms display the 1D distribution of the signal before thresholding after FFE and after 2D distortion.

proposed algorithm in a bandwidth-limited IMDD system using a 47 GHz SiP modulator in the O-band over 2 km of standard single-mode fiber (SSMF); featuring a net throughput of more than 250 Gbps/λ PAM4 and PAM6 below the 6.7% overhead (OH) hard-decision forward error correction (HD-FEC) using linear equalization followed by the proposed 2D distortion approach.

II. 2D Constellation Distortion

Bandwidth-limited IMDD systems require strong equalization at the receiver to reduce the ISI and compensate for the degradation of the received signal bandwidth; however, this converts the additive white Gaussian noise (AWGN) into colored noise. Assuming a transmitted signal $s\,(t)$ through a bandwidth-limited IMDD system with channel response $h\,(t)$, the received signal $q\,(t)$ can be described by:

$$q\,(t) = s\,(t) * h\,(t) + n(t) \tag{1}$$

where $n(t)$ is AWGN, $(*)$ denotes the convolution operation, and $h\,(t)$ acts as a low-pass filter due to the bandwidth-limited components. Thus, equalizing the signal is essential to recover the high-frequency components of the transmitted signal and remove the ISI. The output of an equalizer with transfer function $e(t)$ can be expressed as:

$$q_e(t) = q(t) * e(t) = s(t) * h(t) * e(t) + n(t) * e(t) \tag{2}$$

Given that $E(t)$ is ideally the inverse of $h(t)$ assuming zero ISI as in zero-forcing equalization, $q_e(t)$ can be rewritten as:

$$q_e(t) = s(t) + n(t) * e(t) \tag{3}$$

Therefore, the received signal after ideal equalization is the transmitted signal in addition to colored noise because of the high-pass filtering effect of $e(t)$, which is commonly referred to as equalizer-enhanced in-band noise. The colored noise induces a non-Gaussian distribution of the noise at the receiver. Fig. 1(a) shows the received eye diagram of a 135 Gbaud PAM4 signal. Fig. 1(b) shows the 2D constellation obtained by time-interleaving of consecutive symbols after linear equalization, with the inset presenting the histogram of the equalized signal. The asymmetric variances of the constellation clusters are due to the correlated noise, and the degree of asymmetry is proportional to the equalization depth [15]. It is worth noting that the colored noise and the AWGN noise are indistinguishable in 1D representation; that is why this impairment might be overlooked in IMDD systems.

In this context, we propose a 2D constellation distortion method that reshapes the constellation to minimize the impact of the colored noise, resulting in considerable reduction in the BER. The proposed method uses a 2D function to correct the time-interleaved 2D constellation without rotating or changing the decision thresholds. We utilized a pre-defined 2D function $F\,(x, y)$ that can be described as follows (4), as shown at the bottom of the page, where M is the number of constellation points in 2D (i.e. 16 for PAM4). A denotes the amplitude of each of the 2D Gaussian distributions, $\mu_{\mathrm{x_i}}$ and $\mu_{\mathrm{y_i}}$ are the real and imaginary parts of the i^{th} constellation point, respectively. σ_{x}^2 and σ_y^2 are the variances of the Gaussian distributions along the real and imaginary axes, respectively. θ_i is the inclination angle of the i^{th} cluster of the received signal with respect to the real axis of the IQ plane, and is approximated by $\theta_{\mathrm{i}} \approx \tan^{-1}(\sigma_{y_i}^2 \big/ \sigma_{x_i}^2)$. For simplicity, we set the amplitude of all the Gaussian distributions to A, which is optimized empirically for each symbol rate. $F\,(x, y)$ is a sum of rotated Gaussians with asymmetric variances, which matches the nature of the received 2D constellation. Each constellation point is enveloped by two 2D Gaussian distributions with opposite amplitude signs and displaced in different directions as illustrated in Fig. 1(c). For a received symbol after time-interleaving $R\,[n] = x_n + y_n j$ such that $x_n = x[2n-1]$ and $y_n = x[2n]$, the output after the 2D constellation distortion is given by:

$$R'\,[n] = R\,[n] \mp F\,(x_n, y_n) \pm F\,(x_n, y_n) \cdot j \tag{5}$$

The $\pm$ sign depends on the value of θ or the direction of inclination. $F\,(x, y)$ can be created blindly with $\theta = 45^0$, $\sigma_x^2 = \sigma_y^2 = 0.5$. However, better results are obtained through using a short sequence of the received signal for extracting the signal statistics in terms of the inclination of each cluster θ_{i}, and the mean and variance along the real (μ_{xi}, σ_{xi}^2) and imaginary (μ_{yi}, σ_{yi}^2) axes; so that the 2D distortion can efficiently correct other system impairments as modulator nonlin-

$$F\,(x, y) = \sum_{i=1}^{M} Ae^{-\frac{\left(\left(x-\mu_{xi}-\sigma_x^2\right)sin\theta_i-\left(y-\mu_{yi}+\sigma_y^2\right)cos\theta_i\right)^2}{2\sigma_y^2}} e^{-\frac{\left(\left(y-\mu_{yi}+\sigma_y^2\right)sin\theta_i+\left(x-\mu_{xi}-\sigma_x^2\right)cos\theta_i\right)^2}{2\sigma_x^2}}$$
$$- Ae^{-\frac{\left(\left(x-\mu_{xi}+\sigma_x^2\right)sin\theta_i-\left(y-\mu_{yi}-\sigma_y^2\right)cos\theta_i\right)^2}{2\sigma_y^2}} e^{-\frac{\left(\left(y-\mu_{yi}-\sigma_y^2\right)sin\theta_i+\left(x-\mu_{xi}+\sigma_x^2\right)cos\theta_i\right)^2}{2\sigma_x^2}} \tag{4}$$

ear transfer function and bias-point drifting. This approach is multiplication-free and requires a single addition operation per received symbol, where the 2D distortion map is predefined in a look-up table. Fig. 1(b-d) depict the received 135 Gbaud PAM4 2D constellation after 101 taps FFE (BER $= 5.3 \times 10^{-3}$), the generated $F(x, y)$, and the 2D constellation after distortion (BER $= 3.1 \times 10^{-3}$). Fig. 1(e) show the noise power spectral density (PSD) before and after the proposed 2D distortion; the noise PSD is effectively whitened after 2D distortion. The insets display the histogram of the signal in 1D before thresholding. The 2D constellation distortion whitens the noise PSD and reduces its variance before thresholding, which reduces the BER by more than 40%.

III. Experimental Setup and Digital Signal Processing

Fig. 2 shows the experimental setup and the DSP blocks used at the transmitter and the receiver. At the transmitter, pseudorandom binary sequence (PRBS) is generated and mapped to the desired PAM order. The signal is upsampled to 2 samples per symbol and a raised cosine (RC) filter is used for pulse shaping. A pre-emphasis filter pre-compensates the frequency response of the arbitrary waveform generator (AWG) and the RF amplifier up to 70 GHz. The sampled digital signal is loaded to the AWG (Keysight M8199A) at 256 GSa/s. The AWG output feeds a 60 GHz 3-dB bandwidth and 23-dB gain RF amplifier. The output of the amplifier is directly applied to the SiP modulator using a 67 GHz probe. The transmitter DSP does not include any nonlinear pre-compensation unlike our previously reported results [5]; thus, any nonlinearity within the received signal is generated from the system response. Optically, O-band external cavity laser set to 1302.8 nm launches 13 dBm into the SiP grating couplers and the modulator. A detailed description of the traveling wave Mach-Zehnder modulator (TW-MZM) is presented in [15], [16]. It is characterized by 5.4 dB propagation loss, and a 5.4 V DC Vπ and 47 GHz 3-dB electro-optic bandwidth at 3 V reverse bias. The grating couplers' back-to-back coupling loss is 7.5 dB. Hence, a praseodymium-doped fiber amplifier (PDFA) is used to boost the signal power before a 70 GHz photodetector (PD). Practically, reducing the coupling loss using edge couplers and employing a PD with a transimpedance amplifier (TIA) is a more cost-effective solution and can dispense the PDFA for 2 km reach. The photodiode output is captured by a 110 GHz real-time oscilloscope (RTO) at a sampling rate of 256 GSa/s. Eventually, the receiver DSP is carried out offline, which includes re-sampling to 2 samples per symbol, synchronization, and FFE or VNLE. After the equalization, the output symbols are time-interleaved to apply the proposed 2D constellation distortion. Then, the time-interleaving process is reversed before symbol de-mapping and BER calculations. For the sake of comparison, a two-tap post filter optimized for each symbol rate followed by MLSD is employed; which resembles the conventional way to tackle equalizer-enhanced in-band noise despite its computational complexity. The high-bandwidth transmitter and receiver RF chains imply that the frequency response of the system is mainly limited by the bandwidth of the SiP modulator. The inset of Fig. 2 shows the received electrical spectrum of 140 Gbaud PAM4 signal after 2 km before equalization, which shows more than 20 dB attenuation at 70 GHz.

IV. Results

In this section, we evaluate the proposed approach to tackle equalizer-enhanced in-band noise for two widely used

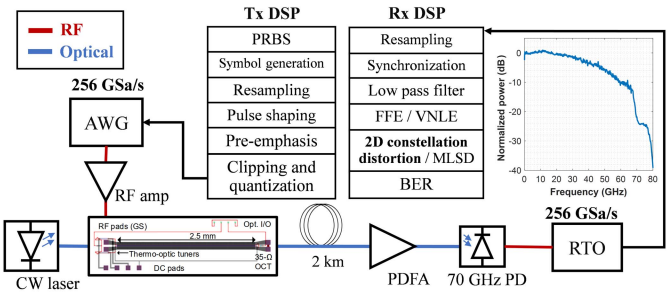

Fig. 2. Experimental setup with the DSP applied at the transmitter and receiver.

equalizers: (1) FFE with 101 taps, and (2) 3rd order VNLE with memory lengths of 101, 3, and 5 for linear, second-order and third-order kernels; further increasing the number of the kernels improves the BER negligibly. The bandwidth-limited IMDD system depicted in Fig. 2 is tested for 2 km transmission. The SiP modulator is reverse biased at 3 V to have a bandwidth of 47 GHz, which is smaller than the transmitted signal bandwidth for all the symbol rates reported in this work. We limit the input to the RF amplifier to operate below the 1-dB Compression point to preserve the linearity and quality of the signal. The peak-to-peak voltage driving the modulator is set to 3.2 V, which maximizes the SNR. The received optical power is set to 7.5 dBm for all the results presented in this section. Fig. 3(a-b) show the achieved BER at different symbol rates for PAM4 and PAM6, respectively. The performance of linear FFE (solid lines) and VNLE (dashed lines) is compared with and without the proposed 2D constellation distortion and MLSD. The VNLE outperforms the linear FFE due to the nonlinearity induced by the RF amplifier, SiP modulator and the square-law detection. This improvement is more pronounced at lower symbol rates because of the higher signal swing driving the RF amplifier and the SiP modulator. The proposed 2D constellation distortion improves the performance in both cases compared to using the equalizer only case; with more pronounced improvement at higher symbol rates because of the stronger equalization and lower SNR. This indicates the effectiveness of the proposed approach in reducing the equalizer-enhanced colored noise. However, MLSD stands as the best option considering only the BER performance. Fig. 3(a) shows that we transmit 135 Gbaud PAM4 (253 Gbps net rate) over 2 km at a BER below the 3.8×10^{-3} HD-FEC threshold, owing to the proposed 2D constellation distortion and the high-bandwidth transmitter RF chain. Fig. 3(b) shows the BER performance for transmitting PAM6 signals that are constructed from the standard 32QAM constellation. The BER reduction because of the proposed constellation distortion is more pronounced in this case due to the highly packed constellation. In Fig. 3(b), we show successful 2 km transmission at 110 Gbaud (257 Gbps net rate) PAM6 using linear FFE and the 2D constellation distortion under the same HD-FEC BER threshold. Therefore, this work surpasses our previous record throughputs for SiP-based PAM4 and PAM6 transmission [5]. Compared to our previous attempt, this work uses the proposed 2D distortion at the receiver and does not employ any nonlinear pre-distortion at the transmitter side.

Fig. 3(c) shows the percentage of BER reduction for different symbol rates and PAM orders as a function of the number of symbols used in extracting the received signal statistics and generating the 2D map $F(x, y)$. For blind distortion (n $= 0$), the proposed technique improves the BER by more than 20%. Increasing the number of symbols improves the

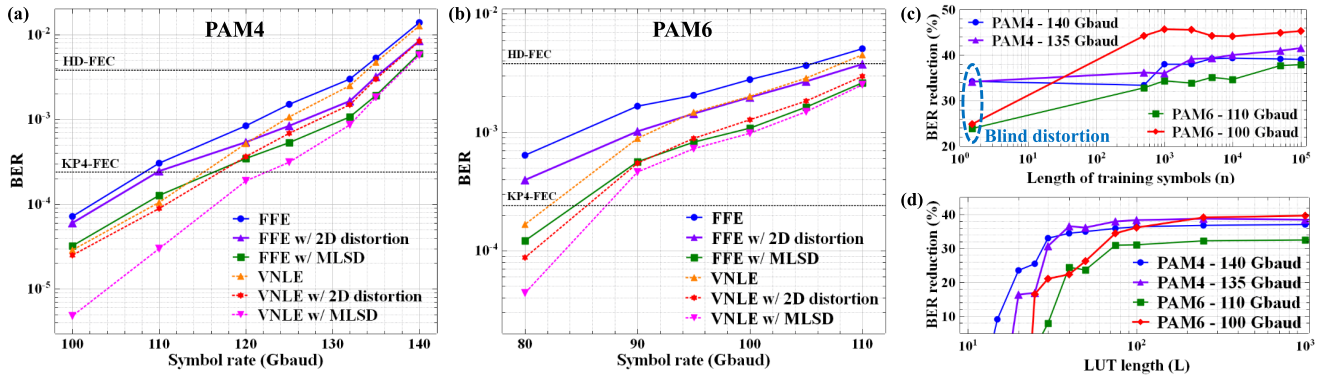

Fig. 3. The BER versus symbol rate for (a) PAM4 and (b) PAM6 after 2 km transmission for different receiver DSP routines. (c) BER reduction versus the number of symbols used in extracting received signal statistics. (d) BER reduction versus the look-up table length.

BER further; however, it saturates beyond 2500 symbols, which is sufficient to have a good estimate of the signal statistics. In the presented results in Fig. 3(a-b), 2500 symbols are used in generating the 2D constellation distortion map. Computationally, the proposed approach requires a single LUT access every 2 symbols and 2 adders that is incomparably simpler than MLSD, considering its different simplified implementations [17]. Fig. 3(d) shows the BER reduction percentage versus the LUT length (L), where the overall LUT has L^2 memory elements. The results show that a LUT length of 25 and 30 is sufficient for having over 30% BER reduction at the reported symbol rates for PAM4 and PAM6, respectively. The larger LUT needed for PAM6 is due to the higher number of constellation points in 2D. Therefore, considering both BER performance and computational complexity, the proposed 2D distortion compromises both metrics and considerably reduces the BER.

V. Conclusion

In conclusion, this work proposes and experimentally evaluates a multiplication-free approach that reduces the impacts of equalizer-enhanced colored noise in bandwidth-limited IMDD systems. The proposed scheme uses a predefined 2D map retrieved from a look-up table to distort the 2D constellation generated from the received signal, which lessens the noise variance before thresholding and results in a considerable BER reduction. The algorithm is evaluated considering a linear FFE or a 3rd order VNLE. Experimental results show the effectiveness of the proposed approach, which allows the transmission of more than 250 Gbps/λ PAM4 and PAM6 net data rate in the O-band over 2 km of SSMF below the 3.8×10^{-3} HD-FEC BER threshold using a 47 GHz SiP modulator and employing the proposed 2D distortion after the linear feed-forward equalizer.

References

[1] G. Price, "Cisco annual internet report (2018–2023) white paper," Cisco, San Jose, CA, USA, Tech. Rep., 2020. [Online]. Available: https://www.cisco.com/c/en/us/solutions/collateral/executive-perspectives/annual-internet-report/white-paper-c11-741490.html

[2] K. Zhong *et al.*, "Experimental study of PAM-4, CAP-16, and DMT for 100 Gb/s short reach optical transmission systems," *Opt. Exp.*, vol. 23, no. 2, pp. 1176–1189, Jan. 2015.

[3] J. Shi, J. Zhang, Y. Zhou, Y. Wang, N. Chi, and J. Yu, "Transmission performance comparison for 100-Gb/s PAM-4, CAP-16, and DFT-S OFDM with direct detection," *J. Lightw. Technol.*, vol. 35, no. 23, pp. 5127–5133, Dec. 1, 2017.

[4] *IEEE Standard for Ethernet—Amendment 10: Media Access Control Parameters, Physical Layers, and Management Parameters for 200 Gb/s and 400 Gb/s Operation*, E. W. Group, New York, NY, USA, 2017.

[5] M. S. Alam, X. Li, M. Jacques, E. Berikaa, P.-C. Koh, and D. V. Plant, "Net 300 Gbps/λ transmission over 2 km of SMF with a silicon photonic Mach–Zehnder modulator," *IEEE Photon. Technol. Lett.*, vol. 33, no. 24, pp. 1391–1394, Dec. 15, 2021.

[6] M. S. Bin Hossain *et al.*, "402 Gb/s PAM-8 IM/DD O-Band EML transmission," in *Proc. Eur. Conf. Opt. Commun. (ECOC)*, Sep. 2021, Paper We1C1.4.

[7] X. Pang *et al.*, "200 Gbps/Lane IM/DD technologies for short reach optical interconnects," *J. Lightw. Technol.*, vol. 38, no. 2, pp. 492–503, Jan. 15, 2020.

[8] F. Zhang, L. Zhang, X. Ruan, F. Yang, H. Ming, and Y. Li, "High baud rate transmission with silicon photonic modulators," *IEEE J. Sel. Topics Quantum Electron.*, vol. 27, no. 3, pp. 1–9, May 2021.

[9] D. Li *et al.*, "180 Gb/s PAM8 signal transmission in bandwidth-limited IMDD system enabled by tap coefficient decision directed Volterra equalizer," *IEEE Access*, vol. 8, pp. 19890–19899, 2020.

[10] K. Zhong *et al.*, "Experimental demonstration of 500 Gbit/s short reach transmission employing PAM4 signal and direct detection with 25 Gbps device," in *Proc. Opt. Fiber Commun., Conf.*, 2015, Paper Th3A.3.

[11] D. Li *et al.*, "Low-complexity equalization scheme for suppressing FFE-enhanced in-band noise and ISI in 100 Gbps PAM4 optical IMDD system," *Opt. Lett.*, vol. 45, no. 9, pp. 2555–2558, 2020.

[12] H. Zhou *et al.*, "Recent advances in equalization technologies for short-reach optical links based on PAM4 modulation: A review," *Appl. Sci.*, vol. 9, no. 11, p. 2342, Jun. 2019.

[13] K. Zhong *et al.*, "140-Gb/s 20-km transmission of PAM-4 signal at 1.3 μm for short reach communications," *IEEE Photon. Technol. Lett.*, vol. 27, no. 16, pp. 1757–1760, Aug. 15, 2015.

[14] T. Wettlin, S. Calabro, T. Rahman, J. Wei, N. Stojanovic, and S. Pachnicke, "DSP for high-speed short-reach IM/DD systems using PAM," *J. Lightw. Technol.*, vol. 38, no. 24, pp. 6771–6778, Dec. 15, 2020.

[15] K. Fukunaga, "Nonwhite observation noise," in *Title: Introduction to Statistical Pattern Recognition*. Amsterdam, The Netherlands: Elsevier, 2013, pp. 128–131.

[16] M. S. Alam *et al.*, "Net 220 Gbps/λ IM/DD transmssion in O-band and C-band with silicon photonic traveling-wave MZM," *J. Lightw. Technol.*, vol. 39, no. 13, pp. 4270–4278, Jul. 1, 2021.

[17] M. Jacques *et al.*, "Net 212.5 Gbit/s transmission in O-band with a SiP MZM, one driver and linear equalization," in *Proc. Opt. Fiber Commun. Conf. Postdeadline Papers*, 2020, Paper Th4A.3.

[18] H. Zamiri-Jafarian and S. Pasupathy, "Complexity reduction of the MLSD/MLSDE receiver using the adaptive state allocation algorithm," *IEEE Trans. Wireless Commun.*, vol. 1, no. 1, pp. 101–111, Jan. 2002.